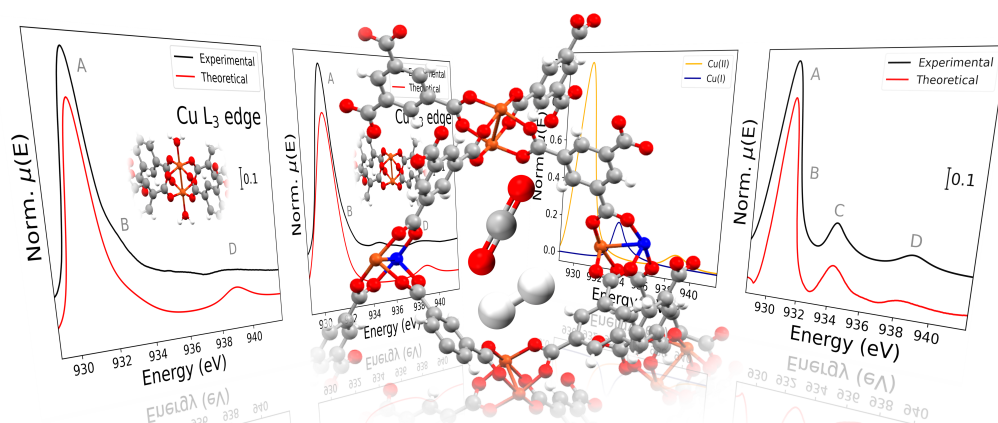


# Graphical Abstract

## Insights into structure and reactivity of MOFs by ambient pressure soft X-ray absorption spectroscopy

Alessandro Tofoni, Francesco Tavani, Luca Braglia, Valentina Colombo, Piero Torelli, Paola D'Angelo



# Insights into structure and reactivity of MOFs by ambient pressure soft X-ray absorption spectroscopy

Alessandro Tofoni<sup>a,\*</sup>, Francesco Tavani<sup>a</sup>, Luca Braglia<sup>b</sup>, Valentina Colombo<sup>c</sup>, Piero Torelli<sup>b</sup>, Paola D'Angelo<sup>a,\*\*</sup>

<sup>a</sup>*Universita' di Roma "La Sapienza", Piazzale Aldo Moro 5, Rome, 00185, Italy*

<sup>b</sup>*CNR-Istituto Officina dei Materiali, TASC, Trieste, 34149, Italy*

<sup>c</sup>*Universita' degli Studi di Milano, Via Golgi 19, Milan, 20133, Italy*

---

## Abstract

Metal-Organic Frameworks (MOFs) are nanostructured porous materials made up by metal cations and organic linkers forming three-dimensional structures. Since their discovery, the local properties of metal centers in MOFs have often been studied with hard X-ray absorption spectroscopy, a powerful bulk-sensitive technique that can hardly provide accurate surface information on these systems. Here, we employ the ambient-pressure soft X-ray absorption spectroscopy, using a newly developed experimental setup, to unveil the formation mechanism of surface defective sites in the prototypical Cu(II)-based MOF HKUST-1, as well as the reactivity and selectivity of these sites towards CO<sub>2</sub> from the analysis of the Cu L<sub>3</sub>-edge near edge X-ray absorption spectroscopy (NEXAFS) data. We observe that, upon thermal heating, Cu(I) defects are formed more abundantly on the surface of the material as compared to the bulk, a process that is almost fully reversed when the MOF is exposed to CO<sub>2</sub>, even when mixed with H<sub>2</sub>. Additionally, we propose a structure and a formation mechanism for such defective sites, supported by theoretical DFT-based calculations.

**Keywords:** MOF, AP-NEXAFS, operando, materials, gas sorption, carbon dioxide

---

\*alessandro.tofoni@uniroma1.it

\*\*p.dangelo@uniroma1.it

## 1. Introduction

A metal-organic framework (MOF) is a material formed by the coordination of polydentate ligands (mostly organic in nature, and often referred to as linkers) to metal ions or clusters (nodes) [1]. Since these materials present three-dimensional porous structures [2, 3] often featuring nanosized apertures and open metal sites [4, 5], they are extremely suitable for applications involving gas-solid interactions, such as heterogeneous catalysis [6, 7] and gas sorption (separation and storage) [8, 9, 10, 11, 12, 13]. In particular, some MOFs have been shown to perform extremely well in the selective capture of CO<sub>2</sub>, due to their high porosity combined with the capability to form coordinatively unsaturated sites (CUSs) throughout the structure [14]. CUSs notably act as strong binding sites [4] for otherwise weakly binding molecules (e. g. CH<sub>4</sub>, H<sub>2</sub> and C<sub>2</sub>H<sub>4</sub>), and they can manifest a preferential interaction with CO<sub>2</sub> in particular cases. Additionally, recent studies have shown that engineering defective sites in UiO-66, a Zr-based MOF, greatly enhances its CO<sub>2</sub> separation selectivity [15], pointing out the pivotal role of defects in this process. HKUST-1, a well-studied MOF made up by Cu<sup>2+</sup> cations and the benzene-1,3,5-tricarboxylate (BTC) linker [16], is known to form defective Cu<sup>+</sup> sites via both thermal [17] and mechanochemical [18] routes. Despite years of debate and thorough research, full consensus on the formation, structure and reactivity of these defective sites is yet to be reached. A clear and final assessment of such properties, especially about the interaction between carbon dioxide (universally regarded as an environmentally harmful species [19]) and the Cu<sup>+</sup> sites would therefore provide crucial information to estimate their impact on CO<sub>2</sub> sorption.

Conventional hard X-ray absorption spectroscopy (XAS) has been widely applied to study the local structural and electronic properties of the metal centers present in MOFs, in general [20], and HKUST-1, in particular [21], but the high degree of penetration possessed by hard X-rays renders this otherwise powerful technique not well suited for determining the properties of surface metal sites. Understanding such properties is fundamental for the full comprehension of the interaction between solid materials and gaseous species, which most importantly happens at a surface level.

In this work, we present a thorough characterization of the defective sites formed in HKUST-1 by thermal heating. Following the considerations above, we employed soft X-ray absorption spectroscopy performed in total electron yield (TEY) mode. TEY mode, combined with the low penetration depth of

38 soft X-rays (few  $\mu\text{m}$ ), renders this technique remarkably surface sensitive ( $<$   
39 10 nm) [22] and suitable for this kind of application. Moreover, we have uti-  
40 lized a recently developed cell capable of performing *operando* AP-NEXAFS  
41 experiments in TEY mode. We have investigated the formation mechanism  
42 and reactivity with  $\text{CO}_2$  and  $\text{H}_2$  of defects in HKUST-1 via *operando* ambient-  
43 pressure X-ray absorption near edge structure (AP-NEXAFS) spectroscopy  
44 experiments and rationalized these findings by theoretical calculations. Such  
45 an approach has already proven succesful for the study of interfacial metal  
46 oxide properties [23, 24], and we believe that it is suited to become a widely  
47 adopted protocol for *operando* experiments on MOFs reactivity in the near  
48 future.

## 49 2. Materials and methods

### 50 2.1. Materials

51 HKUST-1 was purchased at analytical grade from Sigma-Aldrich and  
52 used without further purification. All gaseous reagents ( $\text{He}$ ,  $\text{H}_2$ ,  $\text{CO}_2$ ) were  
53 instead supplied by Linde, with a purity of at least 99.999%.

### 54 2.2. Cu $L_3$ -edge NEXAFS measurements

55 Operando Cu  $L_3$ -edge NEXAFS spectra were recorded using an innovative  
56 reaction cell (described in detail elsewhere [25]) available at the APE-HE  
57 beamline [26] of the Elettra synchrotron radiation facility. This cell can op-  
58 erate at ambient pressure in a temperature range between room temperature  
59 (RT) and 350  $^\circ\text{C}$ . The experiments were performed collecting Cu  $L_3$ -edge  
60 NEXAFS spectra at different temperatures (room temperature and 160  $^\circ\text{C}$ )  
61 and under different gas fluxes ( $\text{He}$ ,  $\text{H}_2$  and  $\text{CO}_2$ ) at 1 bar. 20 mg of the  
62 HKUST-1 MOF powder were pressed into a titanium sample holder which  
63 was then fixed into the reaction cell. The energy scale was calibrated by  
64 simultaneously collecting the Cu  $L_3$ -edge spectrum of a CuO reference dur-  
65 ing the sample measurements, assigning the first maximum of the  $L_3$  edge to  
66 931.9 eV.

### 67 2.3. Theoretical calculations

68 Cu  $L_3$ -edge spectra have been calculated using the FDMNES code [27],  
69 implementing the recently developed sparse solver method [28]. The spec-  
70 tra were calculated using multiple scattering theory including spin-orbit cou-  
71 pling, and the muffin-tin (MT) approximation was used for the potential. The



72 MT radii were chosen to minimize the difference between the potential inside  
 73 the MT spheres and in the interstitial region. All atoms within a cutoff radius  
 74 of 5 Å from the Cu centers have been included in the calculations. The struc-  
 75 tural model used in the calculations regarding the pristine HKUST-1 pad-  
 76 dlewheel unit, along with those pertaining to the  $\text{Cu}^{2+}/\text{Cu}^{2+}$  and  $\text{Cu}^+/\text{Cu}^{2+}$   
 77 dimers resulting from dehydration and dehydration/decarboxylation of the  
 78 pristine unit (see the following section), were built starting from the crystal-  
 79 lographic structure of hydrated HKUST-1 [29]. In this structure, the  $\text{Cu}^{2+}$   
 80 ions are placed at a distance of 3.032 Å and coordinated by five oxygen  
 81 atoms in a square pyramidal configuration. Four of the oxygen atoms belong  
 82 to the BTC linkers and are at a Cu–O distance of 1.852 Å with the apical  
 83 oxygen atom placed at 2.207 Å from the  $\text{Cu}^{2+}$  ion. A cluster containing  
 84 the  $\text{Cu}^{2+}/\text{Cu}^{2+}$  dimer and the four bonded BTC ligands was cut from the  
 85 crystal structure and used as a model for the pristine structure with no fur-  
 86 ther manipulation, while the dehydrated and defective models were obtained  
 87 removing the  $\text{H}_2\text{O}$  molecules and one of the BTC ligands entirely, respec-  
 88 tively. In the dehydrated MOF model, the two  $\text{Cu}^{2+}$  atoms are coordinated  
 89 in a square pyramidal (SP) geometry since all water molecules are removed.  
 90 As far as the defective HKUST-1 model is concerned, one of the two copper  
 91 atoms was reduced to  $\text{Cu}^+$  and the three remaining BTC ligands have been  
 92 kept at the same geometry as the dehydrated model. The  $\text{Cu}^{2+}$  simulated  
 93 spectra were aligned to the experimental data on the basis of the energy of  
 94 the main  $\text{L}_3$ -edge peak. Conversely, the  $\text{Cu}^+$  theoretical spectra were aligned  
 95 to the  $\text{Cu}^+$  peak present in the spectrum of the HKUST-1 sample measured  
 96 in He (50ml/min, 1 bar) at 160 °C. In order to account for the experimental  
 97 resolution, a Gaussian broadening of 0.7 eV was applied to all calculated  
 98 spectra.

### 99 **3. Results and discussion**

100 A comparison between the Cu  $\text{L}_3$ -edge NEXAFS spectrum of pristine  
 101 HKUST-1 collected in He flux (1 bar, 50 mL/min) at room temperature  
 102 and the spectrum collected at 160 °C after thermal treatment for 10 min is  
 103 shown in Figure 1a. In the spectrum collected on the pristine sample, there  
 104 is a main peak at 930.7 eV (peak A, Figure 1a) with a broad shoulder at  
 105 931.9 eV (peak B, 1a) that is completely absent in the spectrum collected  
 106 at 160 °C. Likely, the disappearance of this feature is caused by a change in  
 107 the local copper coordination environment, possibly due to the desorption

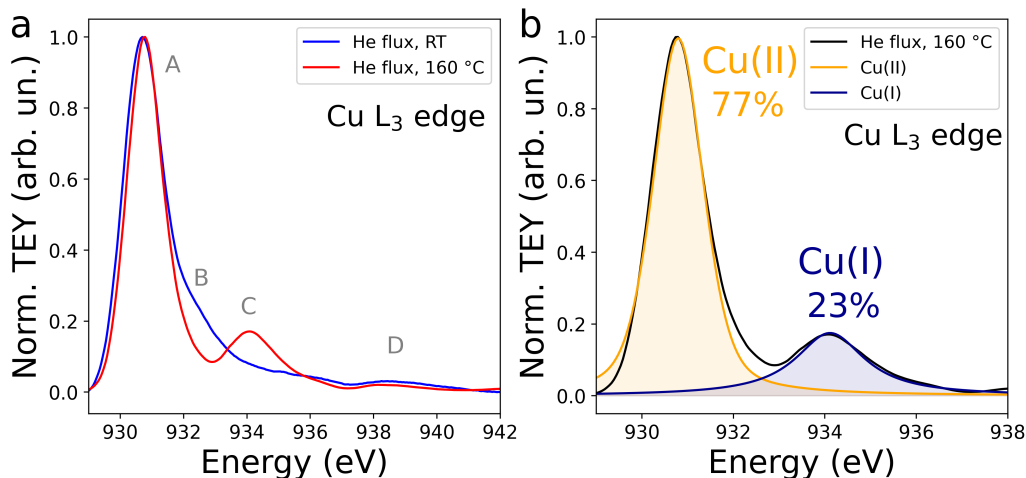


Figure 1: (a) Cu L<sub>3</sub>-edge AP-NEXAFS spectra of HKUST-1 recorded in He (1 bar) at RT (blue line) and in He (1 bar) at 160 °C (red line). The main features are indicated by reference letters (A, B, C and D). (b) Fit of the Cu<sup>2+</sup> (yellow line) and Cu<sup>+</sup> (dark blue line) main peaks in the spectrum recorded in He at 160 °C (black line) using Voigt profiles. The determined relative percentages of Cu<sup>2+</sup> and Cu<sup>+</sup> are reported above the peaks.

of water molecules. The increase in temperature also leads to the formation of a very intense peak at 934.1 eV (peak C, 1a), a value compatible with the white line peak in the Cu L<sub>3</sub>-edge spectrum of Cu<sub>2</sub>O [30], even though the latter spectrum presents a far more asymmetric white line. Such transition is commonly ascribed to a 2p → 3d resonance which, in principle, should not be observed at all as formally the Cu<sup>+</sup> ion is in the 3d<sup>10</sup> electronic configuration. However, it is generally accepted that the Cu<sup>+</sup> ion can show an unusually large partial 3d character in the empty density of states [31] thus allowing this transition to happen. Further, both spectra also present a very broad resonance at about 938.4 eV (peak D, Figure 1a) known to be due to a 2p → 4s electronic transition.

Previous investigations have suggested that mixed valence Cu<sup>+</sup>/Cu<sup>2+</sup> dimers in HKUST-1 can originate either by the reduction of defective clusters [32] or by the reduction of Cu<sup>2+</sup> ions in perfectly coordinated paddle-wheel units [33]. In our mild experimental conditions, it is reasonable to assume that the temperature treatment can provoke the dehydration of pristine Cu<sup>2+</sup>/Cu<sup>2+</sup> paddle-wheel units in the HKUST-1 surface, as well as the formation of defective Cu<sup>+</sup>/Cu<sup>2+</sup> sites. We stress again that AP-NEXAFS

126 investigations performed in TEY mode only probe the first few atomic lay-  
 127 ers, therefore the effects we are observing are limited to the surface of the  
 128 material. The relative surface abundance of the  $\text{Cu}^{2+}$  and  $\text{Cu}^+$  sites can be  
 129 estimated by fitting peaks A and C in the spectrum of defective HKUST-1  
 130 (160 °C, He) via Voigt functions (Figure 1b), and by comparing the integral  
 131 area of the two curves. The calculated ratio was adjusted by the respective  
 132 cross sections of  $\text{Cu}^{2+}$  and  $\text{Cu}^+$  cations, following the procedure reported  
 133 by Fracchia *et al.* [34]. The estimated surface concentration of  $\text{Cu}^+$  sites  
 134 resulted to be 22.7%, which corresponds to a ratio of 45.4% of  $\text{Cu}^+/\text{Cu}^{2+}$   
 135 dimers.

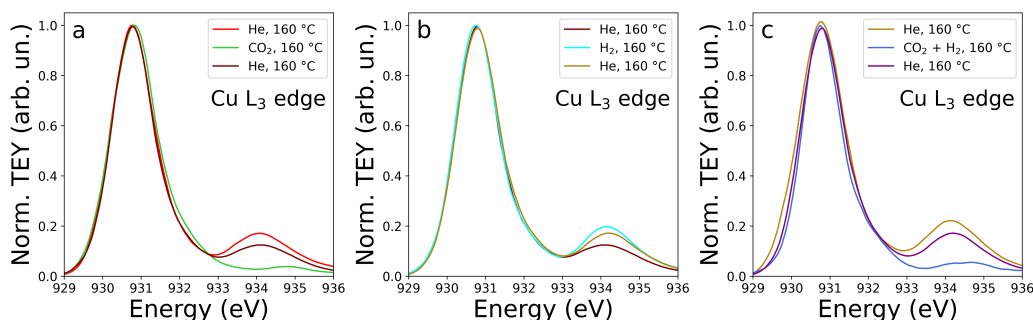


Figure 2: Series of Cu L<sub>3</sub>-edge AP-NEXAFS spectra collected on the HKUST-1 sample: (a) in He flux before and after exposure to CO<sub>2</sub>, and in He flux after purging CO<sub>2</sub> from the sample environment (red, bright green and maroon lines, respectively), (b) in He flux before and after exposure to H<sub>2</sub>, and in pure He flux H<sub>2</sub> afterwards (brown, cyan and olive lines, respectively), (c) in He before, during and after exposure to a gas mixture containing CO<sub>2</sub> (2%) and H<sub>2</sub> (6%) (olive, blue and purple lines, respectively). All spectra were recorded at 160 °C and 1 bar of pressure.

136 After successfully observing the formation of defective sites in HKUST-  
 137 1, we performed additional tests to assess their reactivity and selectivity  
 138 towards two prototypical gas molecules, namely CO<sub>2</sub> and H<sub>2</sub>. Carbon dioxide  
 139 is known to be an oxidant gas but, notably, it has rarely been employed as a  
 140 probe molecule to study metal sites in MOFs.

141 First, we collected the Cu L<sub>3</sub>-edge spectra of defective HKUST-1 before  
 142 and after exposure to a 2% flux of CO<sub>2</sub> at 160 °C, and compared them to the  
 143 spectrum collected at 160 °C in He (Figure 2a). Upon exposure to CO<sub>2</sub>, it  
 144 can be observed that the intensity of peak C is drastically diminished, while  
 145 peak B is not affected. This supports the hypothesis that no water molecules  
 146 are left in the structure, confirming that peak B is the fingerprint of the api-

cal water ligands, and that almost all the  $\text{Cu}^{2+}$  sites are oxidized by carbon dioxide. As soon as the  $\text{CO}_2$  flux is interrupted, however, the intensity of peak C is almost completely restored, proving the reversibility of this process. Conversely, the effect of a 6% flux of  $\text{H}_2$  on the sample previously exposed to  $\text{CO}_2$  at 160 °C is much more limited: the intensity of peak C increases only slightly, as hydrogen promotes the reduction of the  $\text{Cu}^{2+}$  sites, decreasing as soon as the  $\text{H}_2$  flux is stopped (Figure 2b). Finally, we investigated the effect of exposing defective HKUST-1 to a mixture of  $\text{CO}_2$  (2%) and  $\text{H}_2$  (2%) to probe the degree of selectivity of the defective sites towards each gas. In this case, we obtained a spectrum surprisingly similar to that obtained while fluxing only  $\text{CO}_2$  on the defective MOF: peak C is again almost completely absent from the spectrum (Figure 2c), proving that the  $\text{Cu}^+$  sites interact preferentially with  $\text{CO}_2$ . This sequence of spectra further confirms the reversibility of  $\text{CO}_2$  capture by defective HKUST-1 as we observed, once more, an almost complete recovery of peak C upon interruption of the flux.

To rationalize our findings and shed light on the actual structure of the Cu sites in defective HKUST-1, we performed theoretical Cu  $L_3$ -edge calculations using the FDMNES program. The structural models used in these simulations, as well as the employed level of theory, are described in Section 2.3. First, we simulated the spectrum of the pristine MOF using the crystallographic structure of as-prepared HKUST-1. A comparison with the experimental spectrum collected at room temperature in He flux is shown in Figure 3a: the theoretical curve is in very good agreement with the experimental data, as the relative energy position and intensity of peaks A and D are correct and peak B is also nicely reproduced. Next, we calculated a theoretical spectrum using the dehydrated cluster model explained above, where all water ligands have been removed, and compared it to the experimental spectrum collected at 160 °C in  $\text{CO}_2$  flux (Figure 3b) which should only probe non-defective, water-free  $\text{Cu}^{2+}/\text{Cu}^{2+}$  sites. Also in this case the theoretical spectrum is in good agreement with the experimental data: notably, the disappearance of peak B is correctly reproduced by the calculation, confirming that this peak is a fingerprint of the water ligands. In addition, this evidence also proves that the  $\text{CO}_2$ -promoted oxidation of the  $\text{Cu}^+$  sites does in fact happen.

In order to reproduce the experimental spectrum of defective HKUST-1 collected at 160 °C in He flux, we calculated the spectrum of the  $\text{Cu}^+$  centers present in the defective sites using a cluster model containing a  $\text{Cu}^+/\text{Cu}^{2+}$  dimer, shown in Figure 4b. Then, we combined this spectrum in a weighed

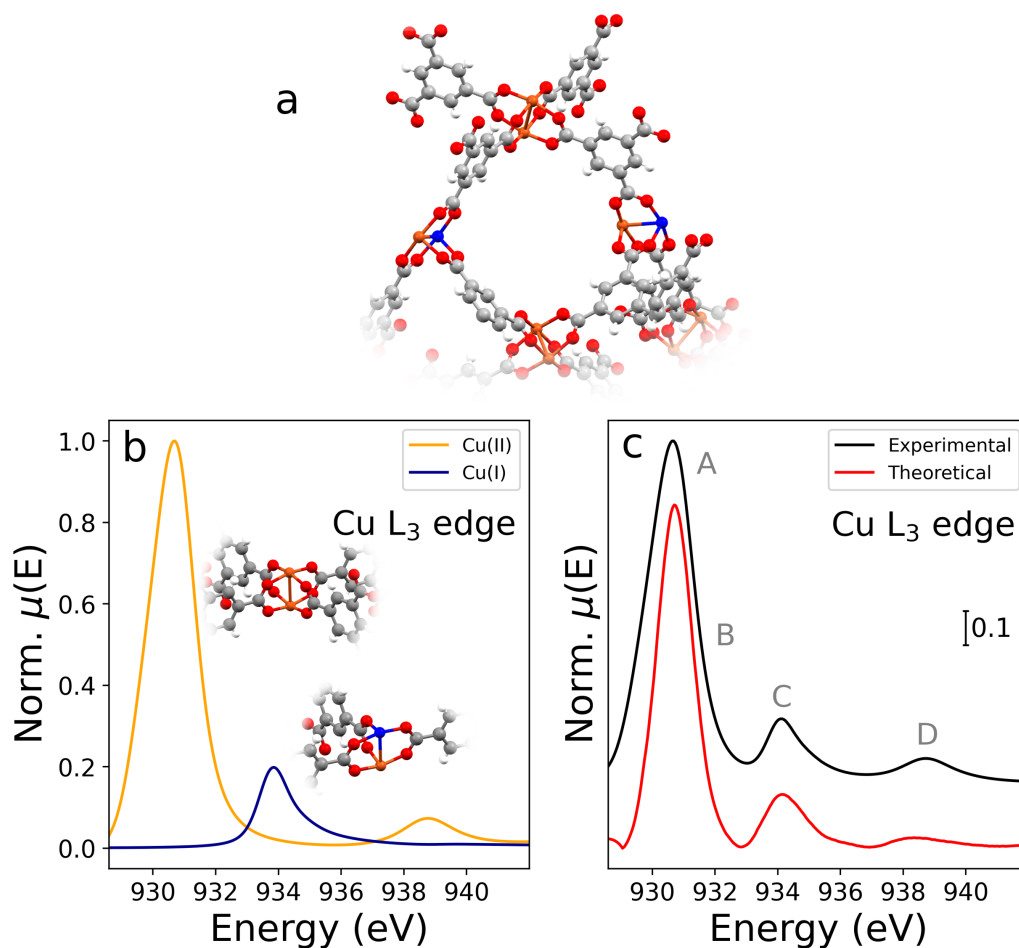


Figure 3: (a) Comparison between the Cu L<sub>3</sub>-edge AP-NEXAFS experimental spectrum relative to the pristine HKUST-1 MOF collected at RT in He flux (black) and the corresponding theoretical calculation (red). (b) Comparison between the Cu L<sub>3</sub>-edge experimental spectrum relative to the pristine HKUST-1 MOF collected at 160 °C while exposing the MOF to CO<sub>2</sub> (black) and the corresponding theoretical calculation (red). The associated molecular clusters are also shown, where the Cu<sup>2+</sup> cation and the oxygen, carbon and hydrogen atoms are depicted in orange, red, grey and white, respectively.

185 sum together with the calculation relative to the Cu<sup>2+</sup> ions within the de-  
 186 hydrated cluster, using the relative surface abundance that we had previ-  
 187 ously determined for each as weigh. The comparison with the experimental  
 188 spectrum collected on HKUST-1 at 160 °C is shown in Figure 4c, and the  
 189 agreement between the experimental and theoretical curves is once again very

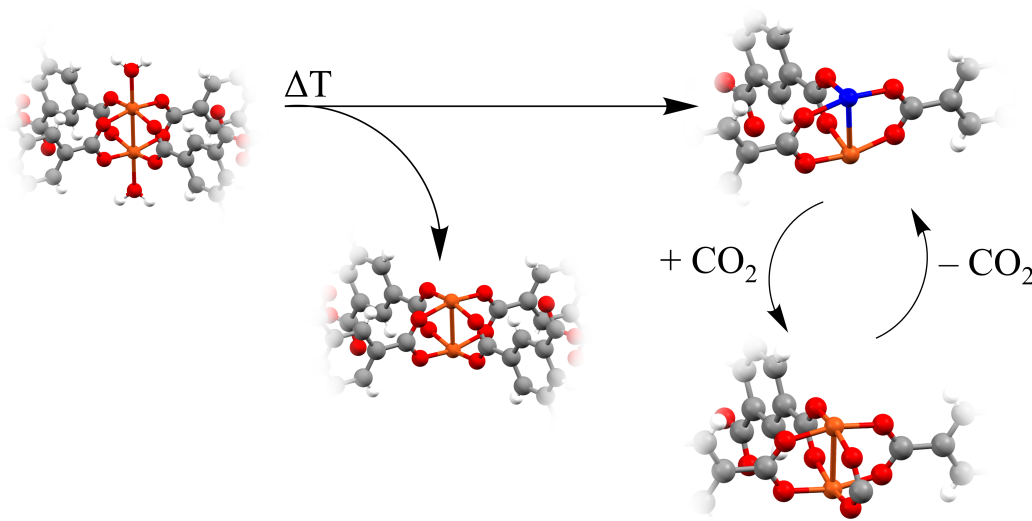


Figure 4: (a) Depiction of the surface copper sites formed upon heating HKUST-1 at 160 °C in He flux. Color code: orange, Cu<sup>2+</sup>; blue, Cu<sup>+</sup>; red, oxygen; grey, carbon; white, hydrogen. (b) Theoretical Cu L<sub>3</sub>-edge spectra calculated for the Cu<sup>2+</sup> (yellow) and Cu<sup>+</sup> (blue) cations present in the Cu<sup>2+</sup>/Cu<sup>2+</sup> and Cu<sup>+</sup>/Cu<sup>2+</sup> dimers, respectively, and weighted by the estimated relative surface abundance. (c) Comparison between the experimental Cu L<sub>3</sub>-edge spectrum collected on HKUST-1 at 160 °C in He flux (black) and the weighted sum of the theoretical spectra belonging to the Cu<sup>2+</sup> and Cu<sup>+</sup> surface species (red).

190 good, confirming our hypothesis for the structure of the defective sites and  
 191 our picture for the overall structure of the thermally heated MOF (shown  
 192 schematically in Figure 4a) where defective sites coexist with coordinatively  
 193 unsaturated paddle-wheels.

194 Finally, the findings we presented thus far allowed us to derive a mechanis-  
 195 tic picture which encompasses the formation mechanism of surface defective  
 196 sites in HKUST-1 and their interaction with CO<sub>2</sub>. A schematic representa-  
 197 tion of this picture is reported in Figure 5: we propose that in the first step  
 198 upon thermal heating the desorption of water molecules from the paddle-  
 199 wheel units occurs, leaving behind coordinatively unsaturated Cu<sup>2+</sup>/Cu<sup>2+</sup>  
 200 dimers. Afterwards, when higher temperatures are reached, a fraction of the  
 201 BTC ligands undergoes a decarboxylation process which in turn causes a  
 202 partial reduction of the dimer to form defective Cu<sup>+</sup>/Cu<sup>2+</sup> sites. These sites  
 203 can then readily interact with CO<sub>2</sub>, which reoxidizes the unit to Cu<sup>2+</sup>/Cu<sup>2+</sup>  
 204 in a process that is completely reversed when the MOF is not exposed to

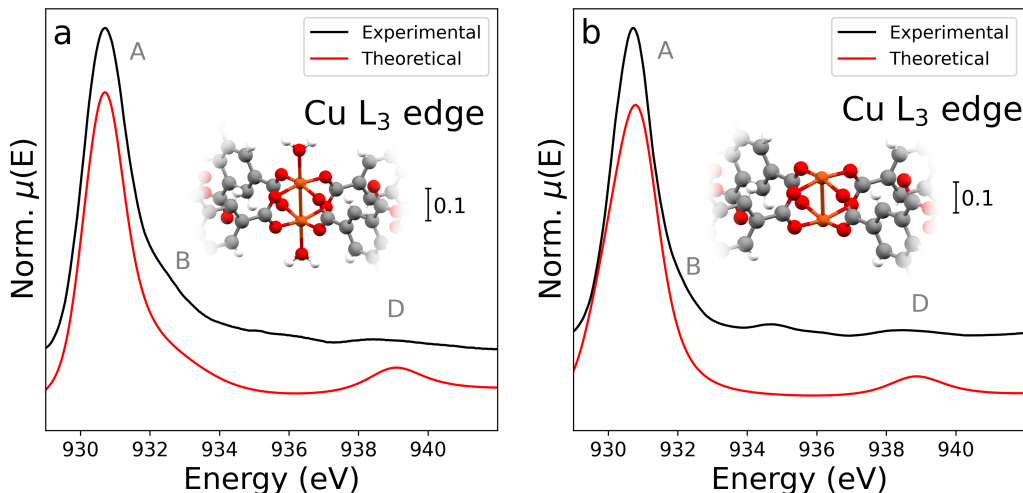


Figure 5: Proposed mechanism for the formation and reactivity of surface defective sites in HKUST-1. Upon heating at 160 °C, water molecules are released from the paddle-wheel units of the pristine MOF. These are converted into coordinatively unsaturated  $\text{Cu}^{2+}/\text{Cu}^{2+}$  dimers which then partially undergo an oxidative decarboxylation of the BTC ligand and yield  $\text{Cu}^+/\text{Cu}^{2+}$  complexes. The  $\text{Cu}^{2+}/\text{Cu}^{2+}$  dimer can then be reversibly replenished upon exposure of the  $\text{Cu}^+/\text{Cu}^{2+}$  sites to  $\text{CO}_2$ . Color code: orange,  $\text{Cu}^{2+}$ ; blue,  $\text{Cu}^+$ ; red, oxygen; grey, carbon; white, hydrogen.

205 carbon dioxide anymore.

## 206 4. Conclusions

207 In this work we highlighted how AP-NEXAFS can provide valuable in-  
 208 formation on the structure and reactivity of MOFs, presenting a thorough  
 209 characterization of the thermally induced properties of surface Cu centers in  
 210 HKUST-1. We also demonstrated how this newly developed technique can  
 211 be combined effectively with theoretical calculations. Cu  $\text{L}_3$ -edge spectra of  
 212 HKUST-1 have been collected at ambient pressure and at room tempera-  
 213 ture and 160 °C, while also varying the gaseous environment ( $\text{He}$ ,  $\text{CO}_2$ ,  $\text{H}_2$ ,  
 214  $\text{CO}_2/\text{H}_2$ ). The structural properties of copper sites present in the first atomic  
 215 layers of HKUST-1 were unveiled, proving also that defective  $\text{Cu}^+/\text{Cu}^{2+}$   
 216 dimeric sites are largely present on the surface of this material. We provided  
 217 evidence of the formation of  $\text{Cu}^+$  surface species upon thermal treatment of  
 218 pristine HKUST-1 at 160 °C, and we estimated that these species account for  
 219 about 45.4% of the total surface Cu content. Further, we have proved that

220  $\text{Cu}^+/\text{Cu}^{2+}$  dimeric units arise from the decarboxylation of the BTC ligands in  
 221 the dehydrated  $\text{Cu}^{2+}/\text{Cu}^{2+}$  dimers, ruling out the formation of  $\text{Cu}^+$  defective  
 222 sites due to the presence of  $\text{Cu}_2\text{O}$  impurities in the MOF, which had been  
 223 previously proposed [35]. Further, we showed that these defective sites can  
 224 be readily and reversibly oxidized by  $\text{CO}_2$ , a molecule which has rarely been  
 225 used as a probe to investigate the surface properties of HKUST-1. We be-  
 226 lieve that the combined experimental and theoretical methodology employed  
 227 in this work can pave the way for the establishment of AP-NEXAFS as a  
 228 routine technique to be employed in the operando characterization of MOFs.

## 229 References

- 230 [1] H. Furukawa, K. E. Cordova, M. O’Keeffe, O. M. Yaghi, The chem-  
 231 istry and applications of metal-organic frameworks, *Science* 341 (2013)  
 232 1230444.
- 233 [2] H. Li, M. Eddaoudi, M. O’Keeffe, O. M. Yaghi, Design and synthesis  
 234 of an exceptionally stable and highly porous metal-organic framework,  
 235 *Nature* 402 (1999) 276–279.
- 236 [3] L. Sun, M. G. Campbell, M. Dincă, Electrically conductive porous  
 237 metal–organic frameworks, *Angew. Chem. Int. Ed.* 55 (2016) 3566–3579.
- 238 [4] Ü. Kökçam-Demir, A. Goldman, L. Esrafil, M. Gharib, A. Morsali,  
 239 O. Weingart, C. Janiak, Coordinatively unsaturated metal sites (open  
 240 metal sites) in metal–organic frameworks: design and applications,  
 241 *Chem. Soc. Rev.* 49 (2020) 2751–2798.
- 242 [5] J. N. Hall, P. Bollini, Structure, characterization, and catalytic prop-  
 243 erties of open-metal sites in metal organic frameworks, *React. Chem.*  
 244 *Eng.* 4 (2019) 207–222.
- 245 [6] J. Lee, O. K. Farha, J. Roberts, K. A. Scheidt, S. T. Nguyen, J. T.  
 246 Hupp, Metal–organic framework materials as catalysts, *Chem. Soc.*  
 247 *Rev.* 38 (2009) 1450–1459.
- 248 [7] D.-H. Nam, O. S. Bushuyev, J. Li, P. De Luna, A. Seifitokaldani, C.-T.  
 249 Dinh, F. P. García de Arquer, Y. Wang, Z. Liang, A. H. Proppe, C. S.  
 250 Tan, P. Todorović, O. Shekhah, C. M. Gabardo, J. W. Jo, J. Choi, M.-J.  
 251 Choi, S.-W. Baek, J. Kim, D. Sinton, S. O. Kelley, M. Eddaoudi, E. H.



- 252 Sargent, Metal–organic frameworks mediate cu coordination for selective  
253 co2 electroreduction, *J. Am. Chem. Soc.* 140 (2018) 11378–11386.
- 254 [8] J.-R. Li, R. J. Kuppler, H.-C. Zhou, Selective gas adsorption and sepa-  
255 ration in metal–organic frameworks, *Chem. Soc. Rev.* 38 (2009) 1477–  
256 1504.
- 257 [9] N. Nijem, H. Bluhm, M. L. Ng, M. Kunz, S. R. Leone, M. K. Gilles, Cu<sup>1+</sup>  
258 in hkust-1: selective gas adsorption in the presence of water, *Chem.*  
259 *Comm.* 50 (2014) 10144–10147.
- 260 [10] H. W. B. Teo, A. Chakraborty, S. Kayal, Evaluation of CH<sub>4</sub> and CO<sub>2</sub>  
261 adsorption on hkust-1 and mil-101(cr) mofs employing monte carlo sim-  
262 ulation and comparison with experimental data, *Appl. Therm. Eng.* 110  
263 (2017) 891–900.
- 264 [11] L. J. Murray, M. Dincă, J. R. Long, Hydrogen storage in metal–organic  
265 frameworks, *Chem. Soc. Rev.* 38 (2009) 1294–1314.
- 266 [12] H. Kim, S. Das, M. G. Kim, D. N. Dybtsev, Y. Kim, K. Kim, Synthesis of  
267 phase-pure interpenetrated mof-5 and its gas sorption properties, *Inorg.*  
268 *Chem.* 50 (2011) 3691–3696.
- 269 [13] J. Li, P. M. Bhatt, J. Li, M. Eddaoudi, Y. Liu, Recent progress on  
270 microfine design of metal–organic frameworks: structure regulation and  
271 gas sorption and separation, *Adv. Mater.* 32 (2020) 2002563.
- 272 [14] P. D. Dietzel, V. Besikiotis, R. Blom, Application of metal–organic  
273 frameworks with coordinatively unsaturated metal sites in storage and  
274 separation of methane and carbon dioxide, *J. Mater. Chem.* 19 (2009)  
275 7362–7370.
- 276 [15] J. Yan, Y. Sun, T. Ji, C. Zhang, L. Liu, Y. Liu, Room-temperature  
277 synthesis of defect-engineered zirconium-mof membrane enabling supe-  
278 rior CO<sub>2</sub>/N<sub>2</sub> selectivity with zirconium-oxo cluster source, *J. Membr.*  
279 *Sci* 653 (2022) 120496.
- 280 [16] S. S.-Y. Chui, S. M.-F. Lo, J. P. Charmant, A. G. Orpen,  
281 I. D. Williams, A chemically functionalizable nanoporous material  
282 [Cu<sub>3</sub>(TMA)<sub>2</sub>(H<sub>2</sub>O)<sub>3</sub>]<sub>n</sub>, *Science* 283 (1999) 1148–1150.

- [17] L. Braglia, F. Tavani, S. Mauri, R. Edla, D. Krizmancic, A. Tofoni, V. Colombo, P. D’Angelo, P. Torelli, Catching the reversible formation and reactivity of surface defective sites in metal–organic frameworks: An operando ambient pressure-nexafs investigation, *The Journal of Physical Chemistry Letters* 12 (2021) 9182–9187.
- [18] T. Steenhaut, N. Grégoire, G. Barozzino-Consiglio, Y. Filinchuk, S. Hermans, Mechanochemical defect engineering of hkust-1 and impact of the resulting defects on carbon dioxide sorption and catalytic cyclopropanation, *RSC adv.* 10 (2020) 19822–19831.
- [19] J. H. Mercer, West antarctic ice sheet and CO<sub>2</sub> greenhouse effect: a threat of disaster, *Nature* 271 (1978) 321–325.
- [20] S. Hinokuma, G. Wiker, T. Sukanuma, A. Bansode, D. Stoian, S. C. Huertas, S. Molina, A. Shafir, M. Rønning, W. Van Beek, et al., Versatile ir spectroscopy combined with synchrotron xas–xrd: chemical, electronic, and structural insights during thermal treatment of mof materials, *Eur. J. Inorg. Chem.* 2018 (2018) 1847–1853.
- [21] E. Borfecchia, S. Maurelli, D. Gianolio, E. Groppo, M. Chiesa, F. Bonino, C. Lamberti, Insights into adsorption of NH<sub>3</sub> on hkust-1 metal-organic framework: a multitechnique approach, *The Journal of Physical Chemistry C* 116 (2012) 19839–19850.
- [22] M. Abbate, J. Goedkoop, F. De Groot, M. Grioni, J. Fuggle, S. Hofmann, H. Petersen, M. Sacchi, Probing depth of soft x-ray absorption spectroscopy measured in total-electron-yield mode, *Surf. Interface Anal.* 18 (1992) 65–69.
- [23] F. Tavani, M. Fracchia, A. Tofoni, L. Braglia, A. Jouve, S. Morandi, M. Manzoli, P. Torelli, P. Ghigna, P. D’Angelo, Structural and mechanistic insights into low-temperature co oxidation over a prototypical high entropy oxide by cu l-edge operando soft x-ray absorption spectroscopy, *Phys. Chem. Chem. Phys.* 23 (2021) 26575–26584.
- [24] F. Tavani, M. Busato, L. Braglia, S. Mauri, P. Torelli, P. D’Angelo, Caught while dissolving: Revealing the interfacial solvation of the Mg<sup>2+</sup> ions on the mgo surface, *ACS Appl. Mater. Interfaces*. 14 (2022) 38370–38378.

- [25] C. Castán-Guerrero, D. Krizmancic, V. Bonanni, R. Edla, A. Deluisa, F. Salvador, G. Rossi, G. Panaccione, P. Torelli, A reaction cell for ambient pressure soft x-ray absorption spectroscopy, *Rev. Sci. Instrum.* 89 (2018) 054101.
- [26] G. Panaccione, I. Vobornik, J. Fujii, D. Krizmancic, E. Annese, L. Giovannelli, F. Maccherozzi, F. Salvador, A. De Luisa, D. Benedetti, A. Gruden, P. Bertoch, F. Polack, D. Cocco, G. Sostero, B. Diviacco, M. Hochstrasser, U. Maier, D. Pescia, C. H. Back, T. Greber, J. Osterwalder, M. Galaktionov, M. Sancrotti, G. Rossi, Advanced photoelectric effect experiment beamline at elettra: A surface science laboratory coupled with synchrotron radiation, *Rev. Sci. Instrum.* 80 (2009) 043105.
- [27] O. Bunău, Y. Joly, Self-consistent aspects of x-ray absorption calculations, *J. Phys.: Condens. Matter* 21 (2009) 345501.
- [28] S. A. Guda, A. A. Guda, M. A. Soldatov, K. A. Lomachenko, A. L. Bugaev, C. Lamberti, W. Gawelda, C. Bressler, G. Smolentsev, A. V. Soldatov, Y. Joly, Optimized finite difference method for the full-potential xanes simulations: Application to molecular adsorption geometries in mofs and metal–ligand intersystem crossing transients, *J. Chem. Theory Comput.* 11 (2015) 4512–4521.
- [29] A. A. Yakovenko, J. H. Reibenspies, N. Bhuvanesh, H.-C. Zhou, Generation and applications of structure envelopes for porous metal-organic frameworks, *J. Appl. Crystallogr.* 46 (2013) 346–353.
- [30] Y. Wang, S. Lany, J. Ghanbaja, Y. Fagot-Revurat, Y. Chen, F. Soldera, D. Horwat, F. Mücklich, J. Pierson, Electronic structures of  $\text{Cu}_2\text{O}$ ,  $\text{Cu}_4\text{O}_3$ , and  $\text{CuO}$ : A joint experimental and theoretical study, *Phys. Rev. B* 94 (2016) 245418.
- [31] M. Grioni, J. Goedkoop, R. Schoorl, F. De Groot, J. Fuggle, F. Schäfers, E. Koch, G. Rossi, J.-M. Esteve, R. Karnatak, Studies of copper valence states with  $\text{Cu L}_3$  x-ray-absorption spectroscopy, *Physical Review B* 39 (1989) 1541.
- [32] W. Wang, D. I. Sharapa, A. Chandresh, A. Nefedov, S. Heißler, L. Heinke, F. Studt, Y. Wang, C. Wöll, Interplay of electronic and steric effects to yield low-temperature  $\text{CO}$  oxidation at metal single sites

- 349 in defect-engineered hkust-1, *Angew. Chem. Int. Ed.* 59 (2020) 10514–  
350 10518.
- 351 [33] P. St. Petkov, G. N. Vayssilov, J. Liu, O. Shekhah, Y. Wang, C. Wöll,  
352 T. Heine, Defects in mofs: a thorough characterization, *ChemPhysChem*  
353 13 (2012) 2025–2029.
- 354 [34] M. Fracchia, P. Ghigna, T. Pozzi, U. Anselmi Tamburini, V. Colombo,  
355 L. Braglia, P. Torelli, Stabilization by configurational entropy of the cu  
356 (ii) active site during co oxidation on  $\text{mg}_{0.2}\text{co}_{0.2}\text{ni}_{0.2}\text{cu}_{0.2}\text{zn}_{0.2}\text{o}$ , *J. Phys.*  
357 *Chem. Lett.* 11 (2020) 3589–3593.
- 358 [35] C. Prestipino, L. Regli, J. G. Vitillo, F. Bonino, A. Damin, C. Lam-  
359 berti, A. Zecchina, P. Solari, K. Kongshaug, S. Bordiga, Local structure  
360 of framework cu(ii) in hkust-1 metallorganic framework: spectroscopic  
361 characterization upon activation and interaction with adsorbates, *Chem.*  
362 *Mater.* 18 (2006) 1337–1346.